environmental microbiology

Environmental Microbiology (2016) **18**(9), 3057–3072 doi:10.1111/1462-2920.13232

Thiosulfate oxidation by *Thiomicrospira thermophila*: metabolic flexibility in response to ambient geochemistry

J. L. Houghton,[1]* D. I. Foustoukos,[2] T. M. Flynn,[3,4] C. Vetriani,[5] Alexander S. Bradley[1] and D. A. Fike[1]

[1]*Department of Earth and Planetary Sciences, Washington University, St. Louis, MO 63130, USA.*

[2]*Geophysical Laboratory, Carnegie Institution of Washington, Washington, DC 20015, USA.*

[3]*Biosciences Division, Argonne National Laboratory, Lemont, IL 60439, USA.*

[4]*Computation Institution, The University of Chicago, Chicago, IL 60637, USA.*

[5]*Department of Biochemistry and Microbiology and Institute of Earth, Ocean and Atmospheric Sciences, Rutgers University, New Brunswick, NJ 08901, USA.*

Summary

Previous studies of the stoichiometry of thiosulfate oxidation by colorless sulfur bacteria have failed to demonstrate mass balance of sulfur, indicating that unidentified oxidized products must be present. Here the reaction stoichiometry and kinetics under variable pH conditions during the growth of *Thiomicrospira thermophila* strain EPR85, isolated from diffuse hydrothermal fluids at the East Pacific Rise, is presented. At pH 8.0, thiosulfate was stoichiometrically converted to sulfate. At lower pH, the products of thiosulfate oxidation were extracellular elemental sulfur and sulfate. We were able to replicate previous experiments and identify the missing sulfur as tetrathionate, consistent with previous reports of the activity of thiosulfate dehydrogenase. Tetrathionate was formed under slightly acidic conditions. Genomic DNA from *T. thermophila* strain EPR85 contains genes homologous to those in the Sox pathway (*soxAXYZBCDL*), as well as rhodanese and thiosulfate dehydrogenase. No other sulfur oxidizing bacteria containing *sox(CD)$_2$* genes have been reported to produce extracellular elemental sulfur. If the apparent modified Sox pathway we observed in *T. thermophila* is present in marine *Thiobacillus* and *Thiomicrospira* species, production of extracellular elemental sulfur may be biogeochemically important in marine sulfur cycling.

Received 10 February, 2015; accepted 17 January, 2016. *For correspondence: E-mail: jhoughton@levee.wustl.edu; Tel. 63130, 314 935 3589; Fax 314 935 7361.

Introduction

Sulfide oxidation is a critical step in the biogeochemical sulfur cycle and occurs via several complex reaction pathways, some of which are biologically mediated (Jørgensen, 1990; Jørgensen and Bak, 1991; Jørgensen and Nelson, 2004). The stepwise oxidation of sulfide to sulfate can occur via several reactive chemical species of intermediate oxidation state. These intermediates, including elemental sulfur, thiosulfate and polythionates, can be biogeochemically important even when their steady-state concentrations are low (sub-μM) due to rapid, hidden (or "cryptic") recycling (Thamdrup *et al.*, 1994; Canfield *et al.*, 2010). Elemental sulfur and thiosulfate can be oxidized, reduced or disproportionated, resulting in multiple pathways and redox intermediates of the sulfur cycle (Troelsen and Jørgensen, 1982; Jørgensen and Nelson, 2004). However, pathways involving intermediate oxidation states of sulfur have been difficult to quantify, with many complex processes taking place simultaneously in the presence of several available oxidants and reductants (Jørgensen, 1990; Jørgensen and Bak, 1991; Flynn *et al.*, 2014).

Two known enzymatic pathways mediate thiosulfate oxidation: (i) the S_4 Intermediate pathway, which involves production and consumption of polythionates (Kelly *et al.*, 1997), and (ii) the multienzyme Sox pathway (Sox = **s**ulfide **ox**idation) (Friedrich *et al.*, 2001). The S_4 Intermediate pathway appears to be restricted to obligate chemolithotrophic strains within the genus *Thiobacillus* and involves the production of tetrathionate from thiosulfate via tetrathionate synthase (Lu and Kelly, 1988; Meulenberg *et al.*, 1992). This process is likely coupled to enzymes that subsequently split tetrathionate to thiosulfate, sulfate or elemental sulfur (Lu and Kelly, 1988; Pronk *et al.*, 1990; Meulenberg *et al.*, 1992).

The Sox pathway is versatile and has been shown to be active in physiologically diverse organisms, including green sulfur bacteria, purple sulfur bacteria and colorless sulfur bacteria (Friedrich *et al.*, 2001; Sauvé *et al.*, 2007; Welte *et al.*, 2009). Complete thiosulfate oxidation via the Sox pathway results in sulfate as the sole product; however, incomplete pathways in which $Sox(CD)_2$ is absent can result in accumulation of elemental sulfur, either intracellularly (Grimm *et al.*, 2008) or extracellularly (Van Gemerden, 1984; Gregersen *et al.*, 2011). The colorless sulfur bacterium *Thiomicrospira crunogena* is known to use the Sox pathway to perform thiosulfate oxidation to sulfate and elemental sulfur (Scott *et al.*, 2006; Sievert *et al.*, 2008), but also produces tetrathionate under acidic conditions (Javor *et al.*, 1990). The environmental conditions under which these various oxidation states are produced and/or consumed are poorly constrained for *Thiomicrospira thermophila*.

Here, we report new genomic and physiological evidence for a modified Sox pathway functioning in *T. thermophila*; a sulfur-oxidizing gammaproteobacterium found in marine settings and identified as an obligate aerobic chemolithomixotroph that can oxidize sulfide, thiosulfate and elemental sulfur (Kuenen and Tuovinen, 1981; Takai *et al.*, 2004). *Thiobacillus* and *Thiomicrospira* spp. are widespread in marine sediments (Kuenen *et al.*, 1985; Robertson *et al.*, 1992; Brinkhoff and Muyzer, 1997) and in marine geothermal environments (Sievert *et al.*, 2000, 2008), particularly in diffuse flow hydrothermal vents (Brinkhoff and Muyzer, 1997; Huber *et al.*, 2003; Brazelton and Baross, 2010). We investigated thiosulfate oxidation by *T. thermophila* strain EPR85, isolated from a seafloor hydrothermal diffuse flow vent on the East Pacific Rise at 9° N. *T. thermophila* is closely related to the well-studied strain *T. crunogena* XCL-2, which employs a pH-dependent Sox pathway for thiosulfate oxidation (Scott *et al.*, 2006; Sievert *et al.*, 2008) that has been shown to produce (at pH 6.3) elemental sulfur as well as consume it (at pH 8.5) (Javor *et al.*, 1990). However, previous examination of *T. crunogena* could not account for all of the sulfur in the system, suggesting the production of undetermined sulfur products under all pH conditions studied (6.3–8.5). Problems with sulfur mass balance were also present in studies of two closely related strains of *Thiobacillus* that oxidize sulfide to elemental sulfur and sulfate (Stefess *et al.*, 1996). In contrast, studies of *T. thermophila* have indicated that thiosulfate oxidation produced equal concentrations of elemental sulfur and sulfate, accounting for all sulfur in the system (Takai *et al.*, 2004). These inconsistent results suggest that thiosulfate oxidation by the Sox pathway may be more complex than previously thought and may result in the production of as-yet unidentified sulfur products.

In this study we have identified the sulfur oxidation reactions mediated by *T. thermophila* in the context of specific sulfur cycling enzymes found in its genome. Under various culture conditions we replicated both the sulfur balance and imbalances in the studies discussed above, and identified the missing sulfur product as tetrathionate. We report data on the stoichiometry and kinetics of these reactions (Table 1) and provide a genetic context for the mechanisms potentially responsible for thiosulfate oxidation to multiple products in *T. thermophila* EPR85.

Results

Stoichiometry and mass balance

When buffered at the high end of its pH tolerance (8.0), *T. thermophila* mediates complete oxidation of thiosulfate to sulfate with no significant buildup of elemental sulfur in the media (Fig. 1a). Maximum accumulation of moderate amounts of free elemental sulfur (S_8) in the media ($<$150 μM) and Tris-extractable solid elemental (polymeric) sulfur ($<$250 μM) (Supporting Information Table S1) is concurrent with the period of fastest thiosulfate consumption. Dissolved oxygen was not completely consumed during growth (Supporting Information Table S1).

In contrast, growth at pH buffered at the low end of tolerance (pH $\sim$ 5.5) results in accumulation of free elemental sulfur and sulfate in the media, consistent with incomplete thiosulfate oxidation to sulfate. Experimental data (Fig. 1b) suggest that thiosulfate oxidation and elemental sulfur oxidation occur simultaneously, as described by the combination of the chemical reactions (ib) and (ii) from Table 1. Over the course of the whole 8 h experiment, total sulfur, as measured by the sum of known reaction products ($[2 * [S_2O_3] + [SO_4] + [S]$), decreased from approximately 23 to 15 mM (Fig. 1b). Abiotic controls at low pH (3.5–5.6), in media buffered with both citrate buffer and Bis-Tris buffer, show no loss of thiosulfate and concentrations of possible products such as tetrathionate, sulfate, or elemental sulfur were negligible for up to 73 h (Supporting Information Table S2).

Growth in unbuffered media results in a complex combination of reactions that depends on pH. As elemental sulfur accumulates in the media, the stoichiometry is consistent with a combination of incomplete thiosulfate oxidation to sulfate [reactions (ib) and (ii) from Table 1]. During this initial phase, the rate of elemental sulfur oxidation [reaction (ii)] is less than elemental sulfur production [reaction (i)], causing an accumulation of elemental sulfur in the media and a decrease in pH from 7.5 to approximately 6. However, a pronounced change in reaction stoichiometry occurs with the onset of elemental sulfur consumption ($t = 8$ h, Fig. 1c), which corresponds to a threshold pH of 6. Here, total sulfur, as measured by the sum of known reaction products ($[2 * [S_2O_3] + [SO_4] + [S]$),

Table 1. Chemical reactions observed in thiosulfate oxidation by *T. thermophila*.

	Net chemical reactions	Reactions	ΔG (kJ/mole rxn)
(ia)	$S_2O_3^{2-} \rightarrow SO_3^{2-} + E \cdot S$	$S_2O_3^{2-} \xrightarrow{rhd \cdot S} SO_3^{2-} + rhd \cdot S \cdot S$	36.6
		$rhd \cdot S \cdot S \xrightarrow{SoxYZ} rhd \cdot S + SoxYZ \cdot S \cdot S^{1-}$	
(ib)	$S_2O_3^{2-} + 1/2O_2 \rightarrow S + SO_4^{2-}$	$S_2O_3^{2-} \xrightarrow{SoxAX/SoxZY \cdot S^{1-}} SoxYZ \cdot S \cdot S_2O_3^{1-} + 2e^-$	−229.6
		$SoxZY \cdot S \cdot S_2O_3^{1-} + H_2O \xrightarrow{SoxB} SoxZY \cdot S \cdot S^{1-} + SO_4^{2-} + 2H^+$	
(ic)	$S_x^{2-} \rightarrow S_{x-1} + S^{2-}$	$S_x^{2-} \xrightarrow{abiotic} S_x^{-1} + S^{2-}$	
		$SoxZY \cdot S \cdot S^{1-} + 3H_2O \xrightarrow{Sox(CD)_2} SoxZY \cdot S \cdot SO_3^{1-} + 6e^- + 6H^+$	
(ii)	$S + H_2O + 3/2O_2 \rightarrow SO_4^{2-} + 2H^+$	$SoxZY \cdot S \cdot SO_3^{2-} + H_2O \xrightarrow{SoxB} SO_4^{2-} + SoxZY \cdot S^{1-} + 2H^+$	−529.9
(iii)	$SO_3^{2-} + 1/2O_2 \rightarrow SO_4^{2-}$	$SO_3^{2-} \xrightarrow{SoxAX/SoxZY^{1-}} SoxZY \cdot S \cdot SO_3^{1-} + 2e^-$	−266.2
		$SoxZY \cdot S \cdot SO_3^{1-} + H_2O \xrightarrow{SoxB} SO_4^{2-} + SoxZY \cdot S^{1-}$	
(iv)	$2S_2O_3^{2-} + 2H^+ + 1/2O_2 \rightarrow S_4O_6^{2-} + H_2O$	$2S_2O_3^{2-} \xrightarrow{tsd} S_4O_6^{2-} + 2e^-$	−242.5

Inferred enzymes involved in thiosulfate and elemental sulfur oxidation for this study include rhodanese (rhd·S), SoxAX, SoxYZ, SoxB, $Sox(CD)_2$ and thiosulfate dehydrogenase (tsd) as indicated over each reaction. Free energy for the net chemical reaction is given in kJ/mole of reaction, with negative values indicating spontaneous reaction in the direction written.

decreased from approximately 11 to 6 mM over 6 h (Fig. 1c), suggesting production of an additional as-of-yet unaccounted for sulfur product. On the contrary, abiotic controls in unbuffered seawater at pH 6.0–7.9 indicate no change in thiosulfate or sulfate concentrations over the course of 144 h at both 35°C and 4°C (Supporting Information Table S2).

To address the issue of a missing sulfur product(s) in both buffered and unbuffered media, we looked for other sulfur phases that could plausibly be present, including Tris-extractable solid elemental (polymeric S) sulfur, sulfide, polysulfides (here referring to the charged dissolved species S_x^{2-}), and polythionates. Only minimal concentrations (<300 μM) of Tris-extractable solid polymeric sulfur were present and polysulfides were not detected. Sulfide concentrations never exceeded 20 μM (Supporting Information Table S1), with the maximum values coinciding with a peak in elemental sulfur concentration. However, polythionates, primarily in the form of tetrathionate ($S_4O_6^{2-}$), were detected by cyanolysis at concentrations up to 1 mM, with continuous production taking place after pH stopped decreasing (Fig. 2a). The abundance of tetrathionate is sufficient to account for the apparent missing sulfur (5.5 mM total) in this experiment (Fig. 2a) and tetrathionate concentrations never decreased under any experimental conditions examined. Thus, once pH drops below 5.7, metastable tetrathionate is present, elemental sulfur consumption begins, and competition for thiosulfate takes place between reactions (i) and (iv). Similarly, production of tetrathionate occurs in experiments buffered at low pH (5.5) and accounts for the apparent missing sulfur (7.7 mM total) in those experiments (Fig. 2b).

Physiology and growth rate

Specific growth rate of *T. thermophila* correlates with pH throughout our experiments. At pH 8.0, where thiosulfate is oxidized completely to sulfate, the maximal specific growth rate of 0.49 h^{-1} is attained (Fig. 3). Specific growth rate decreases with pH, corresponding to a change in reaction stoichiometry (Fig. 3). In unbuffered media, the progression of reaction (ii) (Table 1) resulted in a decrease in pH due to proton production. In every unbuffered experiment, pH eventually reaches a constant value during the thiosulfate oxidation phase of growth, which is coincident with the proton-consuming onset of tetrathionate production [reaction (iv), Table 1]. This growth phase is characterized by the slowest rates observed (Fig. 3, open symbols).

Sequence analysis of T. thermophila *draft genome*

The genome (estimated length of 2.65 mbp) was partially assembled into 40 contigs, with the largest 20 accounting for 97.6% of the bases of the scaffold assembly. The G + C content of the assembly is 50.3%. For comparison, the *T. crunogena* XCL-2 genome has a total length of 2.43 mbp with a G+C content of 43% (Scott *et al.*, 2006). The lengths of the largest 19 contigs in *T. thermophila* are

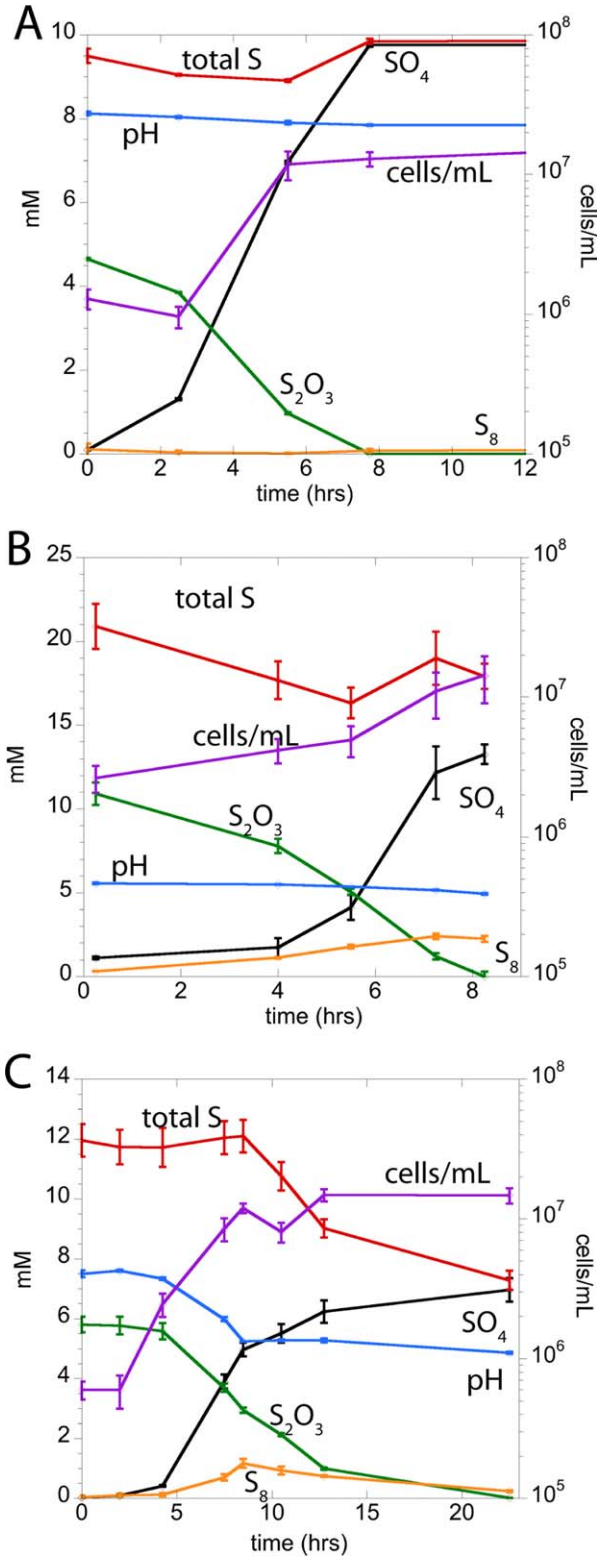

Fig. 1. Time series data for (**A**) thiosulfate oxidation at high pH (8.0) buffered with Tris; (**B**) thiosulfate oxidation at low pH (5.5) buffered with Bis-Tris and (**C**) thiosulfate oxidation in unbuffered media. Error bars based on triplicate experiments are shown for all analyses.

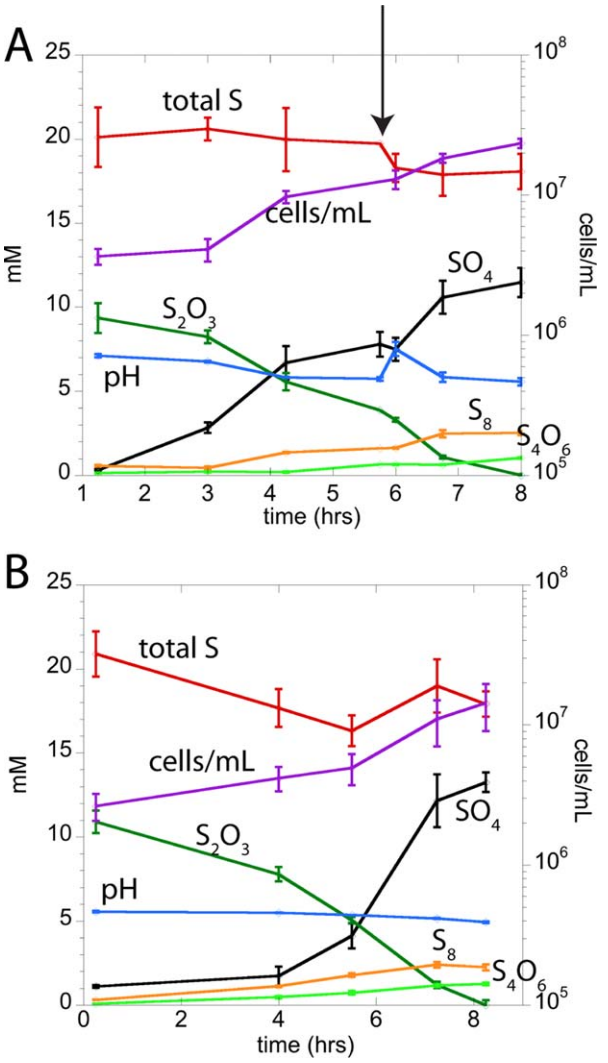

Fig. 2. Stoichiometry of growth experiments including polythionate concentrations determined with the cyanolysis method. (**A**) Growth in unbuffered media follows reactions 1 and 2 until pH drops below 5.5, only below which tetrathionate production (reaction 4) begins. pH was adjusted back to 7.5 at 6 hrs (*arrow*), resulting in a return to reactions (i) and (ii). (**B**) Growth at low pH (5.5; Bis-Tris buffer) occurs with simultaneous production of elemental sulfur, sulfate and tetrathionate via reactions (i), (ii) and (iv) (Table 1). Error bars based on triplicate experiments are shown for all analyses.

indicated in Supporting Information Fig. S1 and are referred to here as nodes, numbered for reference. Sulfur oxidation genes of interest are annotated (Supporting Information Fig. S1).

The genome of *T. thermophila* has homologues for *soxAXZYBCDL*, all of which are necessary for the Sox system to completely oxidize thiosulfate to sulfate. However, in contrast to the well-studied *Paracoccus pantotrophus* (Friedrich *et al.*, 2001), which has all Sox genes clustered in the same region of the genome, *T. thermophila* has homologues of *soxAXYZ* in one cluster and *soxB*, *soxL*

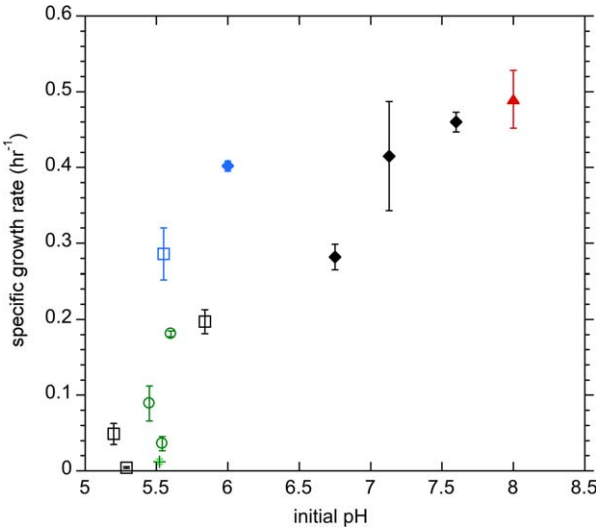

Fig. 3. Specific growth rate as a function of starting pH of the media. Start pH determines which thiosulfate-consuming reaction will be mediated. Highest growth rates are observed when thiosulfate is completely oxidized to sulfate in Tris buffer (pH 8.0) (*solid triangle*) and lowest when thiosulfate is oxidized to tetrathionate (*open squares*), thiosulfate is oxidized to equal parts elemental sulfur and sulfate (*open circles*) or elemental sulfur is oxidized in the absence of thiosulfate (*cross*). Thiosulfate oxidation to elemental sulfur and sulfate with simultaneous oxidation of elemental sulfur to sulfate supports intermediate growth rates (*solid diamonds*). Specific growth rates in Bis-Tris buffer (pH 5.5) are shown in blue; unbuffered media data are shown in *black*; citrate buffer data are shown in *green*.

and *sox(CD)$_2$* in three separate regions (Supporting Information Fig. S1). *T. crunogena* shares this pattern of arrangement (Sievert *et al.*, 2008) and the homologous Sox genes in *T. thermophila* are very closely related to those in *T. crunogena* XCL-2 (Table 2; Scott *et al.*, 2006).

Also like *T. crunogena*, *T. thermophila* has two homologues of rhodanese, a thiosulfate sulfurtransferase specific to thiosulfate as a substrate that cleaves the sulfite moiety and transfers the outer sulfur to an acceptor substrate such as cyanide, lipoic acid or thioredoxin (Smith and Lascelles, 1966; Nandi *et al.*, 2000). Thus, rhodanese could be an alternative enzyme scavenging thiosulfate in *T. thermophila*. The catalytic site in rhodanese binds to both the inner and outer sulfur atoms in thiosulfate in an orientation that polarizes the S—S bond, allowing enzymatic cleavage of the S—S bond (Gliubich *et al.*, 1996). A copy of rhodanese with a completely conserved catalytic site (CRSGQR motif) exists in node 13 of the assembly [Supporting Information Fig. S1; closest relative *T. crunogena* (YP391186), Table 2].

Thiomicrospira thermophila contains additional homologues of genes involved in sulfur-cycling, including sulfide dehydrogenase, which is co-located with *soxB* on the genome, NADPH-dependent sulfite reductase and cytochrome c proteins, sulfide:quinone reductase, and thiosulfate dehydrogenase (Supporting Information Fig. S1). Flavocytochrome-c sulfide dehydrogenase (pfam09242) oxidizes hydrogen sulfide to elemental sulfur coupled to the reduction of cytochrome c (Chen *et al.*, 1994; Visser *et al.*, 1997). The highest-scoring matches for sulfide dehydrogenase are not *T. crunogena*, but *Thioalkalivibrio* sp. ALE20, *Thiomicrospira halophila* and *Chlorobaculum parvum* (Table 2). Sulfite reductase reduces sulfite to hydrogen sulfide coupled to the oxidation of cytochrome c (Crane and Getzoff, 1996). Closest matches for sulfite reductase are *T. crunogena* and *Acinetobacter lwoffii* (Table 2). The sulfide:quinone reductase in *T. thermophila* is homologous to that of *T. crunogena* (Table 2; Supporting Information Fig. S1) that mediates polysulfide formation from hydrogen sulfide by reduction of quinone (Reinartz *et al.*, 1998). *T. thermophila* also has a gene coding for a putative thiosulfate dehydrogenase (Supporting Information Fig. S1) that mediates tetrathionate production from thiosulfate (32.6% similarity to thiosulfate dehydrogenase from *Allochromatium vinosum*; Table 2; Denkmann *et al.*, 2012).

No genes with significant homology to dissimilatory sulfite reductase (*dsr*) or sulfur reductase (*sre*) were identified in the *T. thermophila* genome. These genes could potentially code for enzymes mediating sulfite reduction to hydrogen sulfide and sulfur, or elemental sulfur reduction to hydrogen sulfide, respectively. Homologues for the *sorAB* genes that function as alternatives to the *sox(CD)$_2$* genes (Kappler *et al.*, 2001) to oxidize sulfite to sulfate, were also not found. Homologous genes for thiosulfate reductase (*dvu, phs*; Aketagawa *et al.*, 1985; Bang *et al.*, 2000) that mediate the disproportionation of thiosulfate to sulfite and hydrogen sulfide were not found. Homologous genes for tetrathionate reductase (*ttr*; Hensel *et al.*, 1999) mediating the reduction of tetrathionate to thiosulfate were also not found. However, the failure to identify homologous sequences to these genes in *T. thermophila* does not unequivocally rule out their presence in unaligned portions of the genome (i.e., the genome was not closed).

Discussion

We have demonstrated that in *T. thermophila* strain EPR85 the rate of incomplete thiosulfate oxidation to elemental sulfur and sulfate (reaction ib in Table 1) is decoupled from the rate of elemental sulfur oxidation to sulfate (reaction (ii) in Table 1), with the rate of the latter being a strong function of pH. We have also confirmed that the stoichiometric imbalance of sulfur reported in this study is due to the production of tetrathionate at low pH ($<$6.0). The imbalance previously reported in *Thiomicrospira* and *Thiobacillus* strains is also likely due to tetrathionate production. Analysis of genomic DNA indicates the presence of enzymes for the complete Sox pathway. Based on these findings, we hypothesize that the observed pH

Table 2. Homologous genes for sulfur oxidation enzymes found on the *T. thermophila* genome.

Protein	Node#/position in node	Highest sequence similarity	Nearest neighbor	Comments
SoxA	1 (241316-242146)	YP_390871.1 (1e-180/85.51%)	*T. crunogena XCL-2*	Sulfur oxidation protein with signal peptide and conserved cytochrome c
SoxZ	1 (242251-242589)	YP_390872.1 (1e-62/89.81%)	*T. crunogena XCL-2*	Sulfur oxidation protein (pfam08770)
SoxY	1 (242629-243096)	YP_390873.1 (6e-86/91.61%)	*T. crunogena XCL-2*	Sulfur oxidation protein with signal peptide
SoxX	1 (243134-243508)	YP_390874.1 (2e-81/93.55%)	*T. crunogena XCL-2*	Cytochrome c with signal peptide
Cytochrome c	1 (267914-268273)	YP_390898.1 (3e-57/86.00%)	*T. crunogena XCL-2*	Cytochrome c553 with signal peptide
Hypothetical protein (SoxA)	6 (119648-120526)	YP_003644808.1 (2e-128/66.41%)	*Thiomonas intermedia*	Sulfur oxidation with non-matching signal peptide (KEGG Adeh_2281; KEGG Anaek_1594)
Hypothetical protein (SoxX)	6 (120852-121649)	YP_003644809.1 (4e-38/61.50%)	*Thiomonas intermedia K12*	Sulfur oxidation protein with cytochrome c
rhodanese	6 (165983-166432)	WP_011371372.1 (3e-83/85.71%)	*T. crunogena*	sulfurtransferase
SoxB	5 (107062-108993)	YP_391815.1 (0.0/79.06%)	*T. crunogena XCL-2*	Sulfate thiol esterase UshA with signal peptide, SoxB (cd07411) with metallophosphatase binding site, C-terminal domain (pfam02872)
Sulfide dehydrogenase	5 (129755-131155)	WP_019591503.1 (3e-139/52.18%)	*Thioalkalivibrio sp. ALE20*	NAD(FAD) dependent dehydrogenase with NAD(P) binding domain (cl17500) and flavocytochrome c sulfide dehydrogenase (pfam204176)
SoxC	10 (68564-69925)	YP_390426.1 (0.0/94.48%)	*T. crunogena XCL-2*	Sulfite oxidase with molydopterin-binding domain (cl00199)
SoxD	10 (69906-70994)	YP_390427.1 (0.0/88.69%)	*T. crunogena XCL-2*	Hypothetical protein containing cytochrome c (pfam00034)
		WP_020286444.1 (7e-34/38.89%)	*Osedax symbiont Rs2*	Diheme cytochrome c SoxD (pfam00034)
Sulfide dehydrogenase	9 (44242-45666)	WP_019896075.1 (0.0/79.64%)	*T. halophile*	Hypothetical protein with pyridine nucleotide disulfide oxidoreductase (pfam07992)
		YP_001997639.1 (2e-128/47.10%)	*Chlorobaculum parvum NCIB 8327*	Flavocytochrome c sulfide dehydrogenase (pfam09242)
Sulfite reductase	3 (111050-112147)	YP_392157.1 (0.0/77.81%)	*T. crunogena XCL-2*	Oxidoreductase containing FAD binding domain (pfam00667), cytochrome p450—sulfite reductase (NADPH dependent reduction of SO_3 to H_2S)
Sulfite reductase	4 (51414-53828)	WP_004280698.1 (0.0/39.79%)	*Acinetobacter lwoffii*	Fe-regulated membrane protein PiuB containing CysJ sulfite reductase and flavoprotein with cytochrome p450—sulfite reductase
Sulfide-quinone reductase	2 (33149-34273)	YP_391650.1 (0.0/85.29%)	*T. crunogena XCL-2*	Sulfide-quinone reductase containing pyridine nucleotide—disulfide oxidoreductase (pfam07992)

Table 2. *cont.*

Protein	Node#/position in node	Highest sequence similarity	Nearest neighbor	Comments
Thiosulfate dehydrogenase	16 (13271-14293)	WP_019556080.1 (9e-142/58.88%)	*T. arctica*	Hypothetical protein—hem binding cytochrome c (pfam00034)
		WP_012969337.1 (8e-41/39.41%)	*Allochromatium vinosum DSM180*	Thiosulfate dehydrogenase containing different signal peptide
rhodanese	13 (55570-55866)	YP_391186 (2e-63/95.88%)	*T. crunogena*	Rhodanese-like protein
rhodanese (SoxL)	19 (25750-26430)	YP_003262911 (6e-108/72.64%)	*Halothiobacillus neapolitanus c2*	Rhodanese (pfam PF00581)
		YP_003444124 (7e-59/46.23%)	*Allochromatium vinosum DSM 180*	Sulfurtransferase (SoxL)

Genbank accession number for sequence with highest similarity is shown with corresponding e-value/% similarity in brackets. Known function is included with references to protein families, if known.

dependence of elemental sulfur consumption is consistent with a modified Sox pathway that we outline below, which, if confirmed, represents the first report of elemental sulfur accumulation in bacteria that have genes for *sox(CD)$_2$*.

Thiosulfate consumption

The Sox pathway is a common multienzyme pathway for thiosulfate oxidation found in both photosynthetic purple and green sulfur bacteria and neutrophilic lithoautotrophic sulfur bacteria (Friedrich *et al.*, 2001; Kelly *et al.*, 1997). This pathway requires seven essential proteins (SoxXYZABCD) to complete thiosulfate oxidation to sulfate (Friedrich *et al.*, 2001). The combined activity of the periplasmic SoxYZ, SoxAX and SoxB proteins partially convert thiosulfate to one sulfate (Lu *et al.*, 1985; Wodara *et al.*, 1994; Friedrich *et al.*, 2000, 2001; Welte *et al.*, 2009; Fig. 4; Table 1, enzymatic reaction ib). The remaining enzyme-attached sulfane group is oxidized to a second sulfate by the combined activity of Sox(CD)$_2$ and SoxB proteins (Fig. 4; Wodara *et al.*, 1997; Denger *et al.*, 2008; Quentmeier *et al.*, 2000; Table 1 reaction (ii)). *T. thermophila* strain EPR85 has homologous genes encoding for all the Sox enzymes (*soxAXYZBCD*) needed to completely oxidize thiosulfate to sulfate. Abiotic controls performed at all experimental conditions indicate negligible chemical reaction rates over similar time periods (Supporting Information Table S2) and indicate that the observed differences in thiosulfate oxidation products (e.g., sulfate, elemental sulfur or tetrathionate) are due to microbially mediated reactions. However, our observations of incomplete thiosulfate oxidation to sulfate associated with formation of elemental sulfur at low pH conditions (Fig. 1a and b) suggest that the kinetic rate of thiosulfate oxidation to elemental sulfur (red path in Fig. 4) is enhanced compared with elemental sulfur oxidation to sulfate (blue path in Fig. 4).

Here, we consider a kinetic rate law that describes the net chemical effect of microbial growth via a multienzyme pathway. The rate of thiosulfate consumption was fitted to the following equation:

$$r = kC^q \tag{1}$$

where r is the rate in mmol/h calculated for each timestep, k is the rate constant and q is a constant in h^{-1} (Walas, 1999). The power constant (q) is determined by fitting the rate data for S_2O_3 consumption as a linear function of the concentration of elemental sulfur. In the case where q is not equal to one, the integrated form of Eq. 1 is:

$$k = \frac{C_0^{q-1}}{(t-t_0)(q-1)}\left[\left(\frac{C_0}{C}\right)^{q-1} - 1\right] \tag{2}$$

which can be linearized in the following form:

$$\left(\frac{1}{C}\right)^{q-1} = \left(\frac{1}{C_0}\right)^{q-1} + k(q-1)(t-t_0) \tag{3}$$

Rate data for reaction (i) (Table 1) from four datasets during which thiosulfate reaction to elemental sulfur occurs simultaneously with elemental sulfur oxidation, while mass balance is conserved, were used to determine this constant ($q = 0.421$; Fig. 5a). Thus, the rate of thiosulfate oxidation at all pH conditions tested is not first order, but rather a function of thiosulfate concentration as a power of the concentration of DCM-soluble solid elemental sulfur ($k = 0.207$; Fig. 5b). That time series data from all conditions tested fit the same slope confirms that variable rates of the subsequent reactions (ii) and (iv) in Table 1 do not affect the rate law describing reaction (i) and that the rate is therefore independent of pH. In other words, the mechanism by which thiosulfate is incorporated into the sulfur oxidizing pathway is the rate-limiting step in thiosulfate consumption for *T. thermophila*.

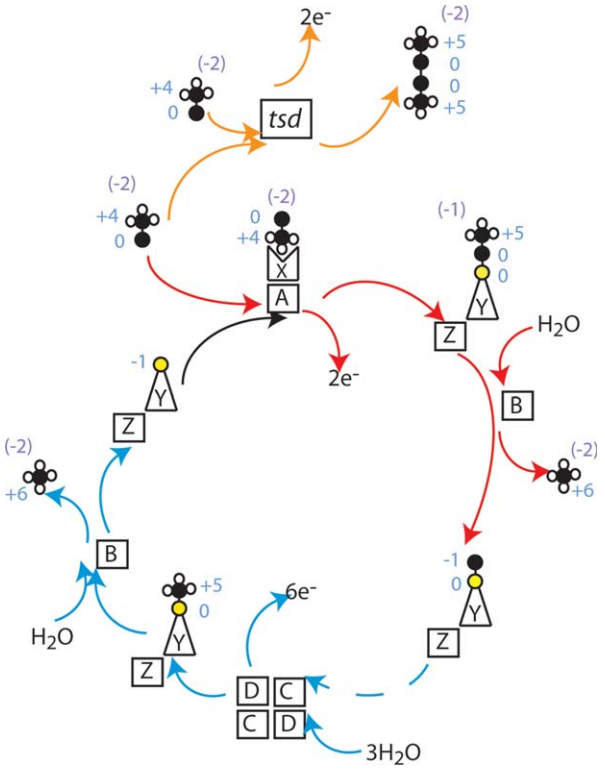

Fig. 4. Variations on the Sox pathway inferred to exist in *T. thermophila* based on this study. When *T. thermophila* is grown buffered at high pH (8.0), sulfur oxidation is consistent with the classic Sox pathway of *P. pantotrophus* (Friedrich *et al.*, 2001), shown here annotated with the oxidation state of each sulfur atom in *blue*. Charged species are indicated in *purple*. In unbuffered experiments once tetrathionate formation begins, the thiosulfate substrate would have to be divided between SoxAX and thiosulfate dehydrogenase to explain the observed chemistry (tsd; *orange arrows*). When grown buffered at low pH (5.5), sulfur oxidation by *T. thermophila*, appears to mediate the second part of the pathway (*blue arrows*) at a slower rate than the first part (*red arrows*), allowing elemental sulfur to accumulate in the media (see text).

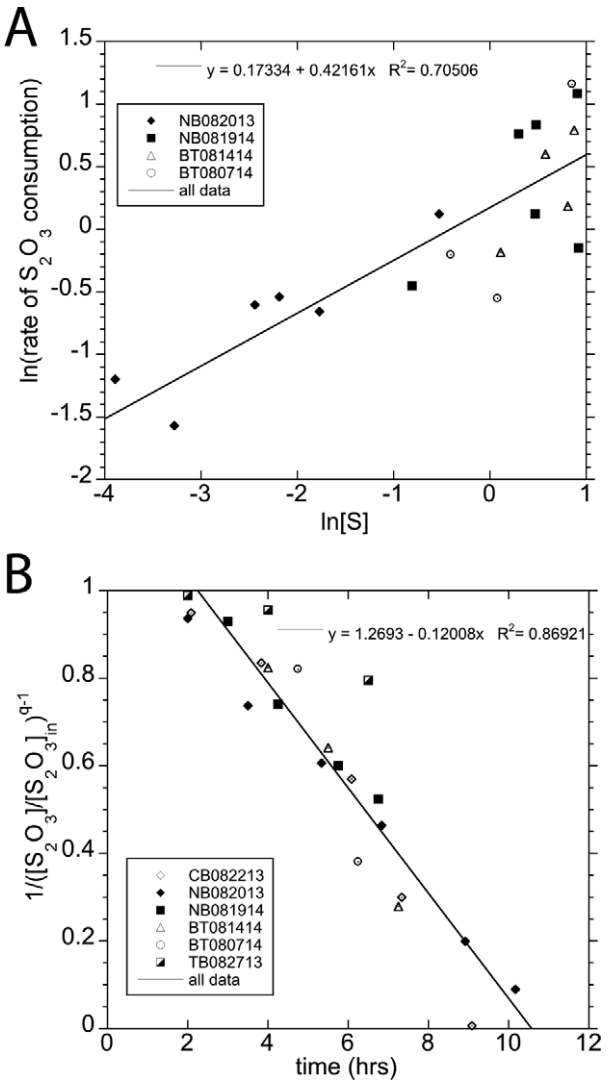

Fig. 5. Rate data during thiosulfate oxidation to elemental sulfur and sulfate. (**A**) The power constant of the rate law is determined by the linear relationship between the log of the rate of thiosulfate consumption and the log of the normalized elemental sulfur concentration, giving a q of 0.421. Initial thiosulfate oxidation rate data [via the simultaneous mediation of reactions (i–iii) in Table 1] from experiments ranging in pH from 7.5 to 5.0, each run in triplicate, were used to determine q. (**B**) The rate constant k for a power law is determined by the linear relationship between $1/[S_2O_3]^{q-1}$ over time. The slope of the linear relationship in this plot corresponds to $k(q-1)$ and the rate constant k for reaction (i) is 0.207.

Elemental sulfur formation

It is thought that the accumulation of elemental sulfur as an intermediate in the Sox pathway only takes place in organisms that lack both Sox(CD)$_2$, which converts the inner sulfur of thiosulfate directly to sulfate, and the *dsr* operon, which oxidizes elemental sulfur to sulfate (Dahl *et al.*, 1993, 2002). In *Allochromatium vinosum*, a rhodanese-like SoxL protein has been implicated in the formation of intracellular sulfur globules, cleaving long chains of polysulfides from SoxYZ [Welte *et al.*, 2009; Table 1 reaction (ib)]. In the case of *T. thermophila* strain EPR85, elemental sulfur is extracellular (Fig. 6). Formation of sulfur globules via a partial Sox pathway has also been observed in colorless sulfur bacteria such as *Beggiatoa* (Mußmann *et al.*, 2007) and members of the *Chlorobiaceae* family of green sulfur bacteria (Gregersen *et al.*, 2011). *T. thermophila* has a homologue of a rhodanese-like enzyme SoxL, but apparently no homologues for the *dsr* genes that would oxidize elemental sulfur (Table 2).

Formation of elemental sulfur by an organism that has genes for the Sox(CD)$_2$ enzyme is unexpected given that pH-dependent inhibition of the activity of Sox(CD)$_2$, responsible for converting the inner sulfur in thiosulfate to sulfate, has not been previously documented. However, it has been shown that the optimal pH for sulfite dehydrogenase activity of the Sox(CD)$_2$ complex is 8.0, with a

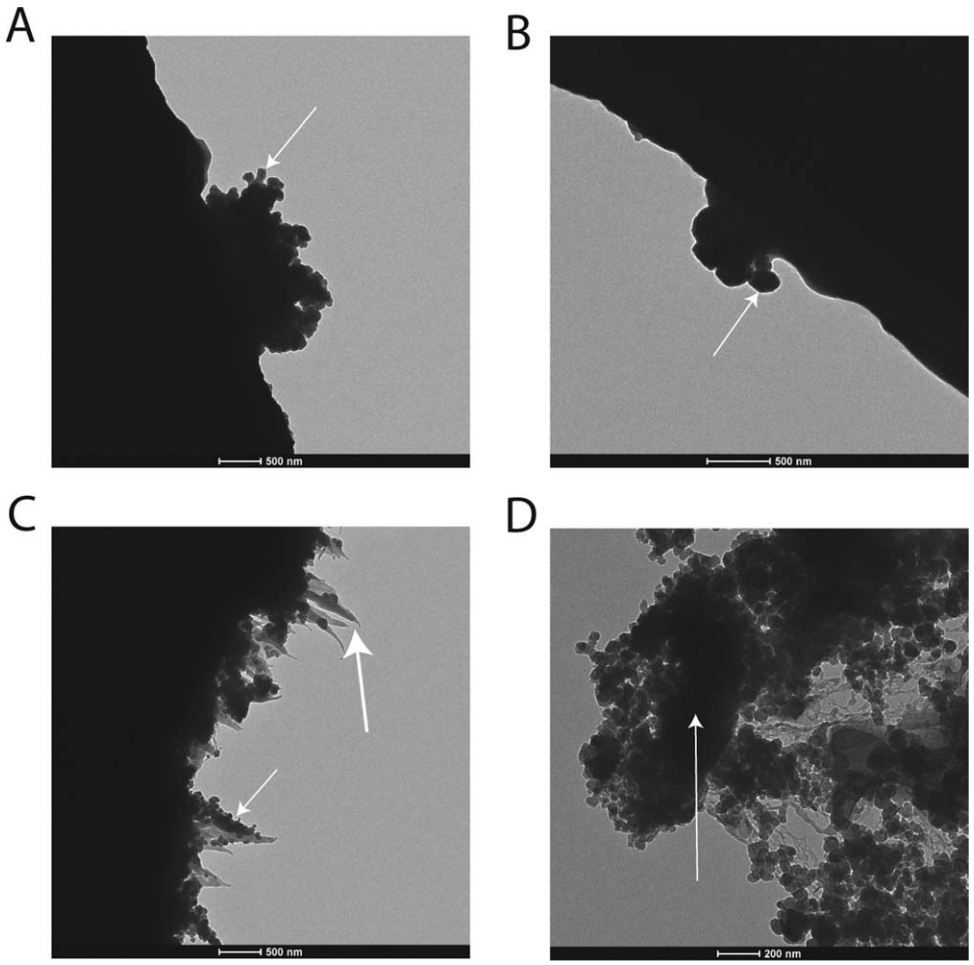

Fig. 6. TEM images of cell pellets with elemental sulfur from the media. (**A**) Small amounts of amorphous elemental sulfur (*arrow*) in the media when grown in Tris buffer at pH 8.0. The smooth edges above and below are the edges of the copper grid on the holder. No biofilm was visible. Scale bar represents 500 nm. (**B**) Crystalline monoclinic elemental sulfur exhibiting a characteristic coffin shape (*arrow*) formed during growth in citrate buffer at pH 5.5. No biofilm was present. Scale bar represents 500 nm. (**C**) Sheets of biofilm trapped in the grid holder, containing nucleating amorphous elemental sulfur (*arrow*), formed after 4 h of growth in unbuffered media. Biofilm (*bold arrow*) appears to effectively trap sulfur and allow growth of larger globules without leading to crystal formation, presumably aiding the cells in re-harvesting the trapped sulfur as other substrates become limiting. Scale bar represents 500 nm. (**D**) A single vibrioid cell (dark shape on the left of the image marked with *arrow*) surrounded by sulfur and imbedded in degrading biofilm network. Note the different scale bar (200 nm). Image taken after 22 h of growth in unbuffered media when sulfur is actively scavenged and tetrathionate is being produced.

10% decline at pH 7.3 and 8.5 (Lu and Kelly, 1984). In addition, the crystal structure of $Sox(CD)_2$ in *Paracoccus pantotrophus* indicates that after the addition of the third oxygen atom onto the SoxY-bound sulfane, the newly created SoxY-S-SO_3^- complex is displaced by OH^-, regenerating the oxidized molybdenum cofactor (Zander *et al.*, 2011). At low pH, this displacement reaction could be inhibited. In addition, given that $Sox(CD)_2$ releases 6 H^+, its activity may be inhibited when pH is already low. Our observations suggest a pH-dependent effect on $Sox(CD)_2$ activity that could also explain the observed elemental sulfur accumulation at low pH observed in *T. crunogena* (Javor *et al.*, 1990) and *Thiobacillus* (Stefess *et al.*, 1996).

In *T. thermophila*, the production of large quantities of extracellular elemental sulfur coincides with low pH and decreased growth rates (Fig. 3). In media buffered at high pH (8.0), the rate of production is inferred to equal consumption such that elemental sulfur does not appreciably accumulate in the media (Fig. 7a). In media buffered at low pH (5.5), elemental sulfur consumption occurs simultaneously with production that always exceeds consumption (Fig. 7b). In unbuffered media initially at pH 7.5, elemental sulfur production and consumption occur simultaneously until pH decreases below 5.5, at which point the rate of consumption exceeds production corresponding to the onset of stationary phase (Fig. 7c). In hydrothermal diffuse flow settings and on chimney surfaces bathed in

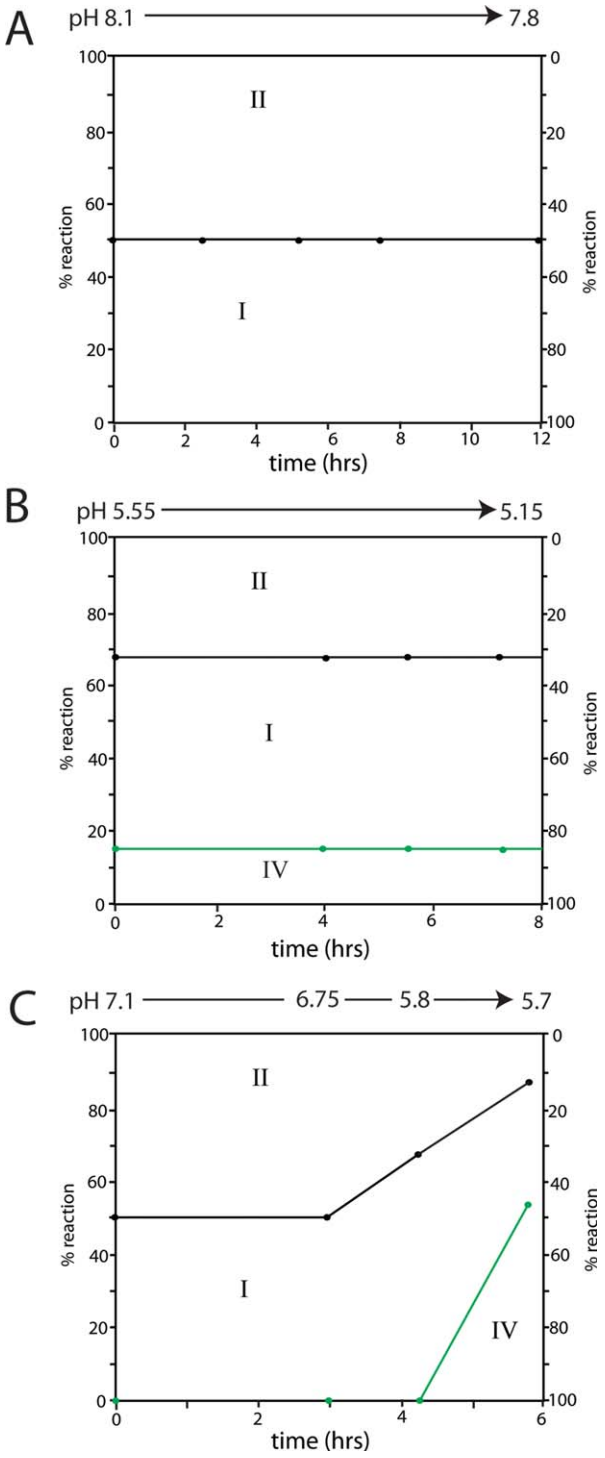

Fig. 7. Schematic depicting the relative degree to which reactions (i), (ii) and (iv) (Table 1) occur over time at various pH conditions (indicated above each figure). Time series progression at high (**A**), low (**B**), and variable (**C**) pH conditions.

hydrothermal fluids diluted with oxygenated seawater where *T. thermophila* is commonly found, these neutral pH values are common, particularly in fluids below 45°C (Foustoukos *et al*., 2009, Ding *et al*., 2005). However, in these environments, turbulent advective flow near chimney orifices frequently results in the outer surfaces of chimneys being subjected to higher temperature and more acidic fluids. Under these conditions, *T. thermophila* can oxidize thiosulfate to elemental sulfur and then maintain cell biomass by utilizing that sulfur.

It is significant that the activity of SoxL is thought to produce polysulfides (Welte *et al*., 2009). Small concentrations (<40 μM) of sulfide are observed to form and remain at constant levels in the media throughout growth experiments buffered at pH 5.5 (Supporting Information Table S1). A mechanism for elemental sulfur formation via a polysulfide precursor may play a role in the creation of extracellular elemental sulfur in a variety of thiosulfate-utilizing bacteria. The exact mechanism for transferring polysulfide to extracellular sulfur globules like those produced by *T. thermophila* is currently unknown. Polysulfides, as charged dissolved species, would be more likely to be excreted extracellularly and rapidly convert to elemental sulfur (initially solid polymeric sulfur and then further to stable S_8 rings) and sulfide (Steudel, 1996). Alternatively, it is possible that polysulfide degrades to elemental sulfur and sulfide in the periplasm and nanocrystalline uncharged elemental sulfur diffuses across the cell membrane as in acidophilic Archaea (Boyd and Druschel, 2013). Our observations in this study are consistent with the nature of either of these mechanisms; however, further study is needed to confirm this.

Tetrathionate production in T. thermophila

Previous studies on thiosulfate oxidation by *Thiobacillus* and *Thiomicrospira* strains have demonstrated variable reaction stoichiometry and mass imbalances suggesting that these bacteria have complex strategies for maintaining growth during variable environmental conditions (Javor *et al*., 1990; Stefess *et al*., 1996). In addition to thiosulfate oxidation, for example, *T. crunogena* changes from elemental sulfur production at pH 6.3 to consumption at pH 8.5 (Javor *et al*., 1990). The sum of products in batch growth of *T. crunogena* was less than the sum of reactants, indicating the presence of additional undetermined sulfur products in previous experiments (Javor *et al*., 1990). Similar discrepancies in sulfur cycling mass balance were observed for two closely related strains of *Thiobacillus* that oxidize sulfide to elemental sulfur and sulfate (Stefess *et al*., 1996). Multiple oxidation pathways of thiosulfate have also been documented in *Allochromatium vinosum*, which variably produces elemental sulfur and sulfate via the Sox pathway or produces tetrathionate at low pH (Hensen *et al*., 2006). Given the similarities in observed stoichiometry and enzymes utilized in thiosulfate oxidation between *A. vinosum* and *T. thermophila*, we investigated the occurrence of

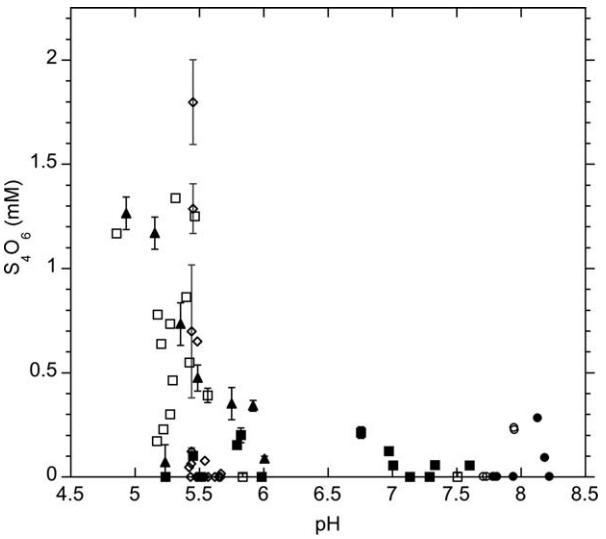

Fig. 8. Inferred and/or measured tetrathionate (see text) as a function of pH in repeat experiments. *Closed symbols* represent composition during exponential growth; *open symbols* are composition during stationary phase. Media tested included unbuffered media (*squares*), Bis-Tris buffer at pH 5.5 (*triangles*), citrate buffer at pH 5.5 (*diamonds*) and Tris buffer at pH 8.0 (*circles*). Measured values are shown with error bars.

tetrathionate to determine if the sulfur imbalance was a result of polythionate formation in *T. thermophila*.

The tetrathionate-producing thiosulfate dehydrogenase of *T. thermophila* closely matches that of *A. vinosum* (Table 2). The purple sulfur bacterium *A. vinosum* has also been shown to oxidize thiosulfate to tetrathionate under neutral to acidic pH conditions using a thiosulfate dehydrogenase (Pott and Dahl, 1998; Hensen *et al*., 2006). In addition, previous studies of *Thiobacillus tepidarius* reported fast rates of tetrathionate production via thiosulfate dehydrogenase (Lu and Kelly, 1988). More importantly, though, a recent review of thiosulfate dehydrogenase genes identified two conserved heme-binding motifs: the necessary catalytic cysteine, and conserved distal ligands that assist in heme-binding (Denkmann *et al*., 2012). The homologous gene in *T. thermophila* shares all conserved regions with only minor substitutions in the heme-binding motifs (Supporting Information Fig. S2).

Below pH 6, *T. thermophila* abruptly switches to tetrathionate production from thiosulfate [Table 1 reaction (iv)], elemental sulfur consumption from the media, and continued processing of thiosulfate to sulfate (Fig. 2a). Comparison of experiments, both with unbuffered and buffered pH (5.5 and 8.0), indicates that this shift in tetrathionate formation correlates with pH (Fig. 8). The stoichiometry of sulfate production indicates that the elemental sulfur lost after this switch cannot account for all sulfate produced (about 1 mM excess SO_4; Fig. 1c); rather, some fraction of thiosulfate consumed must still be processed, albeit at a slow rate. This switch coincides with a change from decreasing to nearly invariant pH in the medium, possibly as a result of simultaneous and comparable reaction rates of elemental sulfur oxidation that consumes H^+ and of tetrathionate production that produces H^+ (reactions (ii) and (iv), Table 1). Given the similarities in reported stoichiometry of thiosulfate oxidation and tetrathionate production in other colorless sulfur bacteria such as *T. crunogena* (Javor *et al*., 1990; Scott *et al*., 2006), *Sulfurimonas denitrificans* (Sievert *et al*., 2008) and *Thiobacillus* strains (Stefess *et al*., 1986), the genetic mechanism responsible for our observations of extracellular elemental sulfur formation and simultaneous tetrathionate production may be more widespread than previously thought.

Conclusions

Thiomicrospira thermophila strain EPR85 has a wide range of metabolic options for coping with the temporal variability in fluid composition that characterizes seafloor diffuse-flow hydrothermal environments. In particular, pH is the dominant control over the type of reactions that are mediated and pH below 5.5 can cause the onset of stationary phase growth, even when thiosulfate is abundant. At pH below 6.0, thiosulfate is oxidized to tetrathionate, accounting for the missing sulfur observed in previous experiments. Thiosulfate is converted to elemental sulfur and sulfate at pH 5.5–8, with the amount of elemental sulfur accumulating in the media increasing as pH decreases. The observed sulfur oxidation chemistry is consistent with the Sox pathway, for which homologues of all genes necessary were found in the genome of *T. thermophila* strain EPR85. The pH dependency of elemental sulfur accumulation suggests a pH-dependent limitation on the activity of $Sox(CD)_2$, resulting in incomplete thiosulfate oxidation. This is the first report of obligate formation of elemental sulfur as an intermediate in an organism that does not contain the *dsr* genes (Grimm *et al*., 2008; Dahl *et al*., 2002).

When pH is lower than 5.5, tetrathionate production is upregulated. *T. thermophila* strain EPR85 has a homologous gene for thiosulfate dehydrogenase, which can mediate tetrathionate production while consuming H^+, partially counteracting the decrease of pH in the medium. Simultaneous with tetrathionate production is the shift to elemental sulfur consumption exceeding production, even if thiosulfate is still present in the media. Thus, *T. thermophila* strain EPR85 can mediate several sulfur oxidation reactions simultaneously, resulting in large geochemical changes with very little increase in biomass.

Experimental procedures

Bacterial strain and growth conditions

Thiomicrospira thermophila strain EPR85 was isolated from fluids collected from a diffuse flow vent on the East Pacific

Rise (EPR; 9°50′N, 104°17′W), at a depth of approximately 2500 m in May 2005 (Cruise AT 11-26, *Alvin* dive 4103). Primary enrichment cultures were initiated shipboard by adding 1 ml of fluids to 10 ml of growth medium designed to enrich for chemolithoautotrophic thiosulfate oxidizing bacteria. The medium used was 142-A (Crespo-Medina *et al.*, 2009). Cultures were incubated at 30°C in the dark. Growth was initially determined by the observation of a change in color of the pH indicator in the medium and then confirmed by direct microscopic counts after staining the cells with acridine orange. For isolation of single colonies, liquid cultures of strain EPR 85 were inoculated on Petri dishes containing medium 142-A solidified with 15 g L^{-1} of noble agar (Sigma). Stocks for long-term storage were prepared by adding 150 μL of 100% sterile glycerol (Fisher Scientific) to 850 μL of overnight cultures, and were stored at −80°C.

In this study, *T. thermophila* strain EPR85 was grown routinely in batch culture with air in the headspace at 35°C on a shaker table. Unbuffered seawater salinity medium contained the following (L^{-1}): 25 g NaCl, 0.2 g NH_4Cl, 1.23 g $MgCl \cdot 6H_2O$, 0.4 g $CaCl_2 \cdot 2H_2O$. After autoclaving, the following filter-sterilized solutions were added (by volume): 10 wt% K_2HPO_4 (0.25 g in 500 ml), 10 wt% $NaHCO_3$ (2.52 g in 500 ml), 1 wt% trace metal solution SL-10, and approximately 6 wt% $Na_2S_2O_3 \cdot 5H_2O$ (16 g in 500 ml). The trace metal solution SL-10 is made as follows (in 1 l): 1.5 g $FeCl_2 \cdot 4H_2O$ dissolved in 10 ml 25% HCl, 70 mg $ZnCl_2$, 100 mg $MnCl_2 \cdot 4H_2O$, 6 mg H_3BO_3, 190 mg $CaCl_2 \cdot 6H_2O$, 2 mg $CuCl_2 \cdot 2H_2O$, 24 mg $NiCl_2 \cdot 6H_2O$, 36 mg $Na_2MoO_4 \cdot 2H_2O$. The thiosulfate stock solution was made fresh often and was not added to media until just prior to inoculation to prevent potential degradation in the media. Bicarbonate, phosphate and trace metals were added just prior to inoculation as well. For the citrate buffer experiments, the salts were added to a buffer base made by mixing 115 ml 0.1 M citric acid with 885 ml 0.1 M sodium citrate. The Bis-Tris buffer was made at 0.1 M and pH was set to the desired value with HCl. The Tris buffer was made by mixing 557 ml 0.1 M Tris-HCl with 443 ml 0.1 M Tris base. The pH was measured prior to inoculation.

Culture stock stored at −80°C was routinely pre-grown in gas-tight serum bottles containing 15 ml unbuffered medium and transferred to 50 ml volumes twice prior to the start of each experiment. The headspace volume in the gas-tight bottles was at least two-third of the total volume to ensure that oxygen gas would not be limiting. The inoculum culture was transferred in exponential growth phase at the start of each experiment to limit the lag phase. Serum bottles were constantly agitated on a Thermo Forma 420 orbital shaker table set at 35°C. Each experiment was grown in triplicate and accompanied by an abiotic control. The abiotic controls never produced any change in thiosulfate concentration, pH or cell abundance.

Analytical techniques

Thiosulfate and sulfate concentrations were monitored by ion chromatography (Metrohm 881) after filtering out biomass and elemental sulfur using an anion column (Metrosep ASupp5-100) with suppression (0.1 M sulfuric acid). Conductivity and UV–Vis detectors (Metrohm 887) were employed in series. The eluent solution was 3.2 mM Na_2CO_3/1 mM $NaHCO_3$ with 2.5 vol% acetone as a modifier. The UV–Vis detector (215 nm) was used exclusively for thiosulfate analysis. Sulfate is not UV-detectable and dissolved species concentrations were analyzed by conductivity detector. The pH was monitored using a Mettler Toledo Ag/AgCl electrode. Sulfide was measured using the method of Cline (1969) as follows: 1 ml sample was fixed with excess Zn acetate (1 ml, 0.3 M); 1 ml of that solution was added to 0.08 ml of mixed diamine reagent, and allowed to sit for up to 1 h; after the color change this solution was diluted to a volume of 12.5 ml with deionized water, transferred to a plastic cuvette and absorbance at 664 nm was analyzed on a UV–Vis spectrometer (Thermo Evolution 60). A blank of sulfide-free media was also fixed in Zn acetate and processed in the same manner. Polythionates and thiosulfate were analyzed by the cyanolysis method (modified from Kelly and Wood, 1994) described in the Supporting Information.

Elemental sulfur (S_8) was extracted from water samples using dichloromethane in glass tubes without letting solvent touch the caps. Three sequential extractions were combined, each with two times the volume of the water sample, to ensure complete extraction. All transfers were made with glass pipettes and quartz cuvettes were used to allow detection in the UV range. The extracted DCM was then measured on a UV–Vis spectrometer (Thermo Evolution 60) by scanning from 200 to 700 nm. Elemental sulfur has a distinctive double peak (Meyer, 1976), which in DCM occurs at 270 and 285 nm. Both peaks are linear with respect to sulfur concentration. The 270 nm peak was chosen because at very low concentrations the 285 nm peak is sometimes indistinct. The scan of a blank (sulfur-free DCM) was subtracted from each sample and the peak height at 270 nm was normalized to the background at 550 nm, as there were differences in baseline in samples analyzed at different times. Polymeric sulfur is insoluble in organic solvents (Steudel and Eckert, 2003). We developed a protocol to measure polymeric sulfur by converting it to DCM-soluble S_8 rings. Based on the stability of commercially available polymeric sulfur (Crystex, Eastman Chemical Company), after the first triple extraction we treated the remaining sample with Tris base (pH 9.4) to raise the pH and provide excess amines in solution. The sample was then autoclaved for 30 min and allowed to sit overnight to promote conversion of polymeric sulfur to stable S_8. Elemental sulfur (S_8) was then quantified after a second triple extraction in DCM. Although we cannot quantify the yield of this process, no insoluble residue was visible after this treatment.

Samples taken for cell counts were fixed in 4 vol% formaldehyde in phosphate buffered saline (PBS: 10.9 g K_2HPO_4, 3.2 g NaH_2PO_4, 90 g NaCl in 1 l DIW) to a dilution factor of 2. Due to the production of elemental sulfur solids in the media, optical density could not be used to determine biomass abundance. Cells were stained with DAPI (2 μl of 1 ppb DAPI in PBS per ml of sample) and allowed to sit for 10 min prior to filtering through 13 mm black polycarbonate 0.22 μm filters (Millipore). Variable volumes (100–400 μl) were carefully pipetted onto a single spot on the filter to concentrate the biomass for imaging. By varying the volume used, the optimal cell density for counting was achieved (<100 cells/field of view). The filters were imaged on a Nikon Eclipse 80i autofluorescence microscope at 1000× magnification. Five to ten representative fields of view were counted and averaged. The cell density

(cells/ml) was adjusted for the factor (f), the volume filtered (v), and the dilution (d) caused by the fixative:

$$C = cfd/v \quad (4)$$

where the fraction (f) is the area of the spot size pipetted onto the filter divided by the area of the field of view counted. Counting with microscopy became difficult once elemental sulfur started forming, as the cells begin to attach and form clumps with the sulfur. As a result the error of counting increases with elemental sulfur concentration, as shown in Supporting Information Fig. S3. Specific growth rates, reported in h^{-1}, were calculated according to:

$$\mu = \ln(X/X_i)/(t - t_i) \quad (5)$$

Separate growth rates were calculated if the reaction stoichiometry shifted during an experiment.

Nucleic acid analysis

Cells were grown in 50 ml unbuffered media and harvested during exponential phase by filtering out excess elemental sulfur through a 5 μm filter before pelleting by centrifugation. Genomic DNA was extracted using the Promega Wizard Genome DNA Purification Kit, following the manufacturer's instructions. Quality and concentration of extracted DNA was verified on a Nanodrop 2000c and by a 2 wt% agar gel to confirm the size and purity of the product.

From the extracted genomic DNA, the 16S DNA sequence was amplified by PCR (Phusion) using the universal bacterial primers 27F (AGAGTTTGATCCTGGCTCAG) and 1492R (GGTTACCTTGTTACGACTT) on an Eppendorf Mastercycler. PCR product was cleaned using the Wizard SV Gel and PCR Cleanup kit (Promega) and the quality of PCR product was confirmed with Nanodrop and by agarose gel. Product was sent to Eurofins MWG Operon for sequencing. To ensure that we had uncontaminated genomic DNA from our strain prior to getting the genome sequenced, we cloned our blunt-end PCR product into a plasmid using the Zero Blunt TOPO PCR cloning kit (Life Technologies) and grew the plasmid in a kanamycin-resistant strain of *E. coli* (OneShot TOP10 Chemically Competent Cells; Life Technologies). The plasmid-bearing *E. coli* was grown on LB broth agar plates dosed with kanamycin at 37°C overnight. Eight single colonies were transferred to 10 ml of LB broth dosed with 10 μl kanamycin and grown on a shaker table at 37°C overnight. The full 10 ml culture was pelleted and the plasmid DNA extracted using the Pure Yield Plasmid Mini Prep System (Promega). Five of these were sent for sequencing and all the sequences aligned against *T. crunogena* XCL-2 as a reference.

Genomic DNA was sent to the Genome Technology Access Center at Washington University School of Medicine for paired-end Illumina sequencing. The first 10 bp from the 5′ end of 101 bp length sequences were clipped from the raw Illumina data. Replicate sequences were removed and the quality of the remaining sequences was confirmed with FastQC (Babraham Bioinformatics). Any sequences with a Phred score of < 30 or a sequence length of < 50 bp were removed using Sickle (Joshi and Fass, 2011). The remaining sequences were assembled using SPAdes (Bankevich *et al.*, 2012) with a range of K-mer lengths (15, 21, 33, 55, 70) tested with very little difference between them when the quality was checked with Quast (Gurevich *et al.*, 2013). The total number of contigs in each assembly ranged from 37 to 40, with L75 score ranging from 9 to 11, and zero uncalled bases. The assembly used has a total length of 2.65 mbp and 40 contigs total, with the largest 20 accounting for 97.6% of the bases of the assembly. The G + C content of the assembly is 50.3%.

The assembly was examined for genes involved in all known sulfur oxidation pathways (MetaCyc) using a series of BLAST queries. These included NADPH-dependent sulfite reductase (EC.1.8.1.2), sulfite oxidoreductase (EC.1.8.2.1), thiosulfate dehydrogenase (EC.1.8.2.2), sulfide dehydrogenase (EC.1.8.2.3), tetrathionate reductase (EC.1.8.5.2), sulfide:quinone reductase (EC.1.8.5.4), dissimilatory sulfite reductase (EC.1.8.99.1), thiosulfate reductase (EC.1.97.1) and rhodanese (EC.2.8.1.1). To confirm those BLAST hits with e value $< 10^{-20}$, the amino acid sequences were compared with the translated amino acid sequence from the assembly. In cases where the closest match was a hypothetical protein, several of the closest matches were examined to determine the homologous gene. In the case of rhodanese, which has been non-selectively annotated in the past, and SoxL, which has only one gene annotated with this identity but is similar to many genes annotated as hypothetical proteins, protein alignments were constructed to confirm the active site motif and conserved regions. In addition, protein alignments were constructed to confirm similarity between multiple genes that gave BLAST hits of the same protein. Global protein alignments with free end gaps were constructed using Blosum62.

Phylogenetic analysis

We obtained a nearly full-length sequence (1514 bp) of the 16S rRNA gene from *T. thermophila* strain EPR85 and, for comparison, *T. crunogena* XCL-2 (Scott *et al.*, 2006). These sequences were aligned to release 117 of the SILVA SSU reference database (Quast *et al.*, 2013) using the SILVA Incremental Aligner (SINA) (Pruesse *et al.*, 2012). This method utilizes a combination of k-mer searching and partial-order alignment to optimize the accuracy of alignment. We then constructed a phylogenetic tree in ARB (Ludwig *et al.*, 2004) of these sequences and other Gammaproteobacteria using the "All-Species Living Tree" Project (LTP) (Yarza *et al.*, 2008; Munoz *et al.*, 2011) as a template. 16S rRNA gene sequences in the LTP are derived from type strains of all classified strains of *Bacteria* and *Archaea*. Tree construction was done using the maximum likelihood algorithm RAxML (Stamatakis, 2006). *T. thermophila* strain EPR85 and *T. crunogena* XCL-2 were inserted into the tree using the ARB parsimony algorithm.

Accession numbers in Genbank

The sequence for the 16S rRNA gene was submitted to GenBank under the accession number KP749905. Sequences for the SoxC and SoxD genes that code for proteins involved in the Sox sulfur oxidation pathway were submitted to GenBank under accession numbers KP749906 and KP749907, respectively.

TEM imaging

To investigate the nature of elemental sulfur produced by *T. thermophila* under different pH conditions, we imaged the sulfur-biomass clusters with a Tecnai Spirit TEM operated at 120 kV with a 2 K 4-megapixel CCD TEM camera. Culture samples at different stages of growth were pipetted (100 μl) onto copper grids, allowing excess water to wick onto a kimwipe. The loaded grid was then stained with methylene blue. Only material that attached to the edge of the grid was visible with this treatment and samples with a high abundance of EPS produced better images as a result.

Acknowledgments

We thank the Genome Technology Access Center in the Department of Genetics at Washington University School of Medicine for help with genomic analysis. The Center is partially supported by NCI Cancer Center Support Grant #P30 CA91842 to the Siteman Cancer Center and by ICTS/CTSA Grant# UL1 TR000448 from the National Center for Research Resources (NCRR), a component of the National Institutes of Health (NIH), and NIH Roadmap for Medical Research. This publication is solely the responsibility of the authors and does not necessarily represent the official view of NCRR or NIH. T.M.F. was supported by the Subsurface Science Scientific Focus Area at Argonne National Laboratory supported by the Subsurface Biogeochemical Research Program, U.S. Department of Energy (DOE) Office of Science, Office of Biological and Environmental Research, under DOE contract DE-AC02-06CH11357. We thank an anonymous reviewer for helpful suggestions that improved this manuscript. We also thank Michael Hügler, K. Adam Bohnert and Melitza Crespo-Medina for technical assistance in the enrichment and isolation of strain EPR 85. This research was supported by funding to D.A.F. and J.H.L from NSF (OCE-1155346; EAR-1124389), to C.V. from NSF (OCE 03-27353, MCB 04-56676 and OCE 11-36451), to D.F. from NSF (OCE 1038114, 1136608 and 1155246) and a Packard Fellowship to D.A.F.

References

Aketagawa, J., Kobayashi, K., and Ishimoto, M. (1985) Purification and properties of thiosulfate reductase from Desulfovibrio vulgaris Miyazaki F. *J Biochem (Tokyo)* **97** (4): 1025–1032.

Bang, S.W., Clark, D.S, and Keasling, J.D. (2000) Engineering hydrogen sulfide production and cadmium removal by expression of the thiosulfate reductase gene (phsABC) from Salmonella enterica serovar typhimurium in Escherichia coli. *Appl Environ Microbiol* **66** (9): 3939–3944.

Bankevich, A., Nurk, S., Antipov, D., Gurevich, A.A., Dvorkin, M., Kulikov, A.S., *et al*. (2012) SPAdes: a new genome assembly algorithm and its applications to single-cell sequencing. *J Comput Biol* **19** (5): 455–477.

Boyd, E.S., and Druschel, G.K. (2013) Involvement of intermediate sulfur species in biological reduction of elemental sulfur under acidic, hydrothermal conditions. *Appl Environ Microbiol* **79** (6): 2061–2068.

Brazelton, W.J., and Baross, J.A. (2010) Metagenomic comparison of two Thiomicrospira lineages inhabiting contrasting deep-sea hydrothermal environments. *PloS One* **5** (10): e13530.

Brinkhoff, T., and Muyzer, G. (1997) Increased species diversity and extended habitat range of sulfur-oxidizing Thiomicrospira spp. *Appl Environ Microbiol* **63** (10): 3789–3796.

Canfield, D.E., Stewart, F.J., Thamdrup, B., De Brabandere, L., Dalsgaard, T., Delong, E.F., *et al*. (2010) A cryptic sulfur cycle in oxygen-minimum–zone waters off the Chilean coast. *Science* **330**: 1375–1378.

Chen, Z.-W., Koh, M., Van Driessche, G., Van Beeumen, J.J., Bartsch, R.G., Meyer, T.E., *et al*. (1994) The structure of flavocytochrome c sulfide dehydrogenase from a purple phototrophic bacterium. *Science* **266**: 430–432.

Cline, J.D. (1969) Spectrophotometric determination of hydrogen sulfide in natural waters. *Limnol Oceanogr*, **14**: 454–458.

Crane, B.R., and Getzoff, E.D. (1996) The relationship between structure and function for the sulfite reductases. *Curr Opin Struct Biol* **66**: 744–756.

Crespo-Medina, M., Chatziefthimiou, A., Cruz-Matos, R., Pérez-Rodríguez, I., Barkay, T., Lutz, R.A., *et al*. (2009) Salinisphaera hydrothermalis sp. nov., a mesophilic, halotolerant, facultatively autotrophic, thiosulfate-oxidizing gammaproteobacterium from deep-sea hydrothermal vents, and emended description of the genus Salinisphaera. *Int J Syst Evol Microbiol* **59**: 1497–1503.

Dahl, C., Kredich, N.M., Deutzmann, R., and Truper, H.G. (1993) Dissimilatory sulphite reductase from *Archaeoglobus fulgidus*: physico-chemical properties of the enzyme and cloning, sequencing and analysis of the reductase genes. *J Gen Microbiol* **139**: 1817–1828.

Dahl, C., Prange, A., and Steudel, R. (2002) Natural polymeric sulfur compounds. In *Biopolymers, Vol. 9: Miscellaneous biopolymers and biodegradation of synthetic polymers*. Steinbüchel, Hrsg., A. (ed). Weinheim: Wiley-VCH, pp. 35–62.

Denger, K., Weinitschke, S., Smits, T.H., Schleheck, D., and Cook, A.M. (2008) Bacterial sulfite dehydrogenases in organotrophic metabolism: separation and identification in Cupriavidus necator H16 and in Delftia acidovorans SPH-1. *Microbiology* **154** (1): 256–263.

Denkmann, K., Grein, F., Zigann, R., Siemen, A., Bergmann, J., van Helmont, S., *et al*. (2012) Thiosulfate dehydrogenase: a widespread unusual acidophilic c-type cytochrome. *Environ Microbiol* **14**: 2673–2688.

Ding, K., Seyfried, W.E.J., Zhang, Z., Tivey, M.K., Von Damm, K.L., and Bradley, A.M. (2005) The in-situ pH of hydrothermal fluids at mid-ocean ridges. *Earth Planet Sci Lett*, **237** (1–2): 167–174.

Flynn, T.M., O'Loughlin, E.J., Mishra, B., DiChristina, T.J., and Kemner, K.M. (2014) Sulfur-mediated electron shuttling during bacterial iron reduction. *Science* **344** (6187): 1039–1042.

Foustoukos, D.I., Seyfried, W.E., Jr., Ding, K., and Pester, N.J. (2009) Dissolved carbon species in associated diffuse and focused flow hydrothermal vents at the Main Endeavour Field, northern Juan de Fuca ridge. *Geochem Geophys Geosyst* **10**: Q10003.

Friedrich, C.G., Quentmeier, A., Bardischewsky, F., Rother, D., Kraft, R., Kostka, S., and Prinz, H. (2000) Novel genes coding for lithotrophic sulfur oxidation of Paracoccus pantotrophus GB17. *J Bacteriol* **182** (17): 4677–4687.

Friedrich, C.G., Rother, D., Bardischewsky, F., Quentmeier, A., and Fischer, J. (2001) Oxidation of reduced inorganic sulfur compounds by bacteria: emergence of a common mechanism?. *Appl Environ Microbiol* **67** (7): 2873–2882.

Gliubich, F., Gazerro, M., Zanotti, G., Delbono, S., Bombieri, G., and Berni, R. (1996) Active site structural features for chemically modified forms of rhodanese. *J Biol Chem* **271** (35): 21054–21061.

Gregersen, L.H., Bryant, D.A., and Frigaard, N.U. (2011) Mechanisms and evolution of oxidative sulfur metabolism in green sulfur bacteria. *Front Microbiol* **2**: 116.

Grimm, F., Franz, B., and Dahl, C. (2008) Thiosulfate and sulfur oxidation in purple sulfur bacteria. In *Microbial Sulfur Metabolism*. Dahl, C., and Friedrich, C.G. (eds). Berlin Heidelberg: Springer, pp. 101–116.

Gurevich, A., Saveliev, V., Vyahhi, N., and Tesler, G. (2013) QUAST: quality assessment tool for genome assemblies. *Bioinformatics* **29** (8): 1072–1075.

Hensel, M., Hinsley, A. P., Nikolaus, T., Sawers, G., & Berks, B. C. (1999). The genetic basis of tetrathionate respiration in Salmonella typhimurium. *Mol Microbiol*, **32** (2): 275–287.

Hensen, D., Sperling, D., Trüper, H.G., Brune, D.C., and Dahl, C. (2006) Thiosulphate oxidation in the phototrophic sulphur bacterium Allochromatium vinosum. *Mol Microbiol* **62** (3): 794–810.

Huber, J.A., Butterfield, D.A., and Baross, J.A. (2003) Bacterial diversity in a subseafloor habitat following a deep-sea volcanic eruption. *FEMS Microb Ecol* **43** (3): 393–409.

Javor, B.J., Wilmot, D.B., and Vetter, R.D. (1990) pH-Dependent metabolism of thiosulfate and sulfur globules in the chemolithotrophic marine bacterium Thiomicrospira crunogena. *Arch Microbiol* **154** (3), 231–238.

Jørgensen, B.B. (1990) A thiosulfate shunt in the sulfur cycle of marine sediments. *Science* **249** (4965): 152–154.

Jørgensen, B.B., and Bak, F. (1991) Pathways and microbiology of thiosulfate transformations and sulfate reduction in a marine sediment (Kattegat, Denmark). *Appl Environ Microbiol* **57** (3): 847–856.

Jørgensen, B.B., and Nelson, D.C. (2004) Sulfide oxidation in marine sediments: geochemistry meets microbiology. *Geol Soc Am Spl Papers* **379**: 63–81.

Joshi, N.A., and Fass, J.N. (2011) Sickle: a sliding-window, adaptive, quality-based trimming tool for FastQ files (Version 1.33) [Software]. URL https://github.com/najoshi/sickle.

Kappler, U., Friedrich, C.G., Trüper, H.G., and Dahl, C. (2001) Evidence for two pathways of thiosulfate oxidation in Starkeya novella (formerly Thiobacillus novellus). *Arch Microb* **175** (2): 102–111.

Kelly, D.P., and Wood, A.P. (1994) Synthesis and determination of thiosulfate and polythionates. *Method Enzymol* **243**: 475–501.

Kelly, D.P., Shergill, J.K., Lu, W.P., and Wood, A.P. (1997) Oxidative metabolism of inorganic sulfur compounds by bacteria. *Anton Van Leeuw* **71** (1-2): 95–107.

Kuenen, J.G., and Tuovinen, O.H. (1981) The genera Thiobacillus and Thiomicrospira. In *The Prokaryotes*. Starr, M.P., Stolp, H., Trüper, H.G., Balows, A., and Schlegel, H.G. (eds). Berlin Heidelberg: Springer, pp. 1023–1036.

Kuenen, J.G., Robertson, L.A., and Van Gemerden, H. (1985) Microbial interactions among aerobic and anaerobic sulfur-oxidizing bacteria. *In Advances in Microbial Ecology*. Marshall, K.C. (ed). New York: Springer, pp. 1–59.

Lu, W.P., and Kelly, D.P. (1984) Properties and role of sulphite: cytochrome c oxidoreductase purified from Thiobacillus versutus (A2). *J Gen Microbiol* **130** (7): 1683–1692.

Lu, W.P., and Kelly, D.P. (1988) Cellular location and partial purification of the 'thiosulphate-oxidizing enzyme'and 'trithionate hydrolyase'from thiobacillus tepidarius. *J Gen Microbiol* **134** (4): 877–885.

Lu, W.P., Swoboda, B.E.P., and Kelly, D.P. (1985) Properties of the thiosulphate-oxidizing multi-enzyme system from *Thiobacillus versutus*. *Biochim Biophys Acta* **828** (2): 116–122.

Ludwig, W., Strunk, O., Westram, R., Richter, L., Meier, H., Buchner, A., *et al*. (2004) ARB: a software environment for sequence data. *Nucleic Acids Res* **32**: 1363–1371.

Meulenberg, R., Pronk, J.T., Hazeu, W., Bos, P., and Kuenen, J.G. (1992) Oxidation of reduced sulphur compounds by intact cells of Thiobacillus acidophilus. *Arch Microbiol* **157** (2): 161–168.

Meyer, B. (1976) Elemental sulfur. *Chem Rev* **76** (3): 367–388.

Munoz, R., Yarza, P., Ludwig, W., Euzéby, J., Amann, R., Schleifer, K.-H., *et al*. (2011) Release LTPs104 of the all-species living tree. *Syst Appl Microb* **34**: 169–170.

Mußmann, M., Hu, F.Z., Richter, M., de Beer, D., Preisler, A., Jørgensen, B.B., *et al*. (2007) Insights into the genome of large sulfur bacteria revealed by analysis of single filaments. *PLoS Biol* **5**: e230.

Nandi, D.L., Horowitz, P.M., and Westley, J. (2000) Rhodanese as a thioredoxin oxidase. *Int J Biochem Cell Biol* **32** (4): 465–473.

Pott, A.S., and Dahl, C. (1998) Sirohaem sulfite reductase and other proteins encoded by genes at the dsr locus of Chromatium vinosum are involved in the oxidation of intracellular sulfur. *Microbiology* **144** (7): 1881–1894.

Pronk, J.T., Meulenberg, R., Hazeu, W., Bos, P., and Kuenen, J.G. (1990) Oxidation of reduced inorganic sulphur compounds by acidophilic thiobacilli. *FEMS Microb Lett* **75** (2): 293–306.

Pruesse, E., Peplies, J., and Glöckner, F.O. (2012) SINA: accurate high-throughput multiple sequence alignment of ribosomal RNA genes. *Bioinformatics* **28** (14): 1.

Quast, C., Pruesse, E., Yilmaz, P., Gerken, J., Schweer, T., Yarza, P., *et al*. (2012) The SILVA ribosomal RNA gene database project: improved data processing and web-based tools. *Nucleic Acids Res* **41**: D590–D596.

Quentmeier, A., Kraft, R., Kostka, S., Klockenkämper, R., and Friedrich, C.G. (2000) Characterization of a new type of sulfite dehydrogenase from Paracoccus pantotrophus GB17. *Arch Microb* **173** (2): 117–125.

Reinartz, M., Tschäpe, J., Brüser, T., Trüper, H.G., and Dahl, C. (1998) Sulfide oxidation in the phototrophic sulfur bacterium Chromatium vinosum. *Arch Microb* **170** (1): 59–68.

Robertson, L.A., Kuenen, J.G., Balows, A., Truper, H.G., Dworkin, M., Harder, W., and Schleifer, K.H. (1992) The colorless sulfur bacteria. *The Prokaryotes: A Handbook on the Biology of Bacteria: Ecophysiology, Isolation, Identification, Applications*, Vol. **I**, 2nd ed. Balows, A., Truper, H., Dworkin, M., Harder, W., and Schleifer, K.H. (eds). New York: Springer, pp. 385–413.

Sauvé, V., Bruno, S., Berks, B.C., and Hemmings, A.M. (2007) The SoxYZ complex carries sulfur cycle intermediates on a peptide swinging arm. *J Biol Chem* **282** (32): 23194–23204.

Scott, K.M., Sievert, S.M., Abril, F.N., Ball, L.A., Barrett, C.J., Blake, R.A., *et al*. (2006) The genome of deep-sea vent chemolithoautotroph Thiomicrospira crunogena XCL-2. *PLoS Biol* **4**: e383.

Sievert, S.M., Hügler, M., Taylor, C.D., and Wirsen, C.O. (2008) Sulfur oxidation at deep-sea hydrothermal vents. In *Microbial Sulfur Metabolism*. Dahl, C., and Friedrich, C.G. (eds). Berlin Heidelberg: Springer, pp. 238–258.

Sievert, S.M., Kuever, J., and Muyzer, G. (2000) Identification of 16S ribosomal DNA-defined bacterial populations at a shallow submarine hydrothermal vent near Milos Island (Greece). *Appl Environ Microbiol* **66** (7): 3102–3109.

Smith, A.J., and Lascelles, J. (1966) Thiosulphate metabolism and rhodanese in Chromatium sp. strain D. *J Gen Microbiol* **42** (3): 357–370.

Stamatakis, A. (2006) RAxML-VI-HPC: maximum likelihood-based phylogenetic analyses with thousands of taxa and mixed models. *Bioinformatics* **22** (21): 2688–2690.

Stefess, G.C., Torremans, R.A.M., De Schrijver, R., Robertson, L.A., and Kuenen, J.G. (1996) Quantitative measurement of sulphur formation by steady-state and transient-state continuous cultures of autotrophic Thiobacillus species. *Appl Microbiol Biotechnol* **45** (1–2): 169–175.

Steudel, R. (1996) Mechanism for the formation of elemental sulfur from aqueous sulfide in chemical and microbiological desulfurization processes. *Ind Eng Chem Res* **35**: 1417–1423.

Steudel, R., and Eckert, B. (2003) Solid sulfur allotropes. In *Elemental Sulfur and Sulfur-Rich Compounds I, Topics in Current Chemistry*. Steudel, R. (ed). Berlin Heidelberg: Springer, pp. 1–80.

Takai, K., Hirayama, H., Nakagawa, T., Suzuki, Y., Nealson, K.H., and Horikoshi, K. (2004) Thiomicrospira thermophila sp. nov., a novel microaerobic, thermotolerant, sulfur-oxidizing chemolithomixotroph isolated from a deep-sea hydrothermal fumarole in the TOTO caldera, Mariana Arc, Western Pacific. *Int J Syst Evol Microbiol* **54** (6): 2325–2333.

Thamdrup, B., Fossing, H., and Jørgensen, B.B. (1994) Manganese, iron and sulfur cycling in a coastal marine sediment, Aarhus Bay, Denmark. *Geochim Cosmochim Acta* **58** (23): 5115–5129.

Troelsen, H., and Jørgensen, B.B. (1982) Seasonal dynamics of elemental sulfur in two coastal sediments. *Estuar Coast Shelf Sci* **15** (3): 255–266.

Van Gemerden, H. (1984) The sulfide affinity of phototrophic bacteria in relation to the location of elemental sulfur. *Arch Microbiol* **139** (4): 289–294.

Visser, J.M., de Jong, G.A., Robertson, L.A., and Kuenen, J.G. (1997) A novel membrane-bound flavocytochrome c sulfide dehydrogenase from the colourless sulfur bacterium Thiobacillus sp. W5. *Arch Microbiol* **167** (5): 295–301.

Walas, S.M. (1999) Reaction kinetics. In *Perry's Chemical Engineers' Handbook*, 7th ed. Perry, R.H. and Green, D.W. (eds). New York: McGraw-Hill.

Welte, C., Hafner, S., Krätzer, C., Quentmeier, A., Friedrich, C.G., and Dahl, C. (2009) Interaction between Sox proteins of two physiologically distinct bacteria and a new protein involved in thiosulfate oxidation. *FEBS Lett* **583** (8): 1281–1286.

Wodara, C., Bardischewsky, F., and Friedrich, C.G. (1997) Cloning and characterization of sulfite dehydrogenase, two c-type cytochromes, and a flavoprotein of Paracoccus denitrificans GB17: essential role of sulfite dehydrogenase in lithotrophic sulfur oxidation. *J Bacteriol* **179** (16): 5014–5023.

Wodara, C., Kostka, S., Egert, M., Kelly, D.P., and Friedrich, C.G. (1994) Identification and sequence analysis of the soxB gene essential for sulfur oxidation of Paracoccus denitrificans GB17. *J Bacteriol* **176** (20): 6188–6191.

Yarza, P., Richter, M., Peplies, J., Euzeby, J., Amann, R., Schleifer, K.-H., *et al*. (2008) The All-Species Living Tree project: A 16S rRNA-based phylogenetic tree of all sequenced type strains. *Syst Appl Microbiol* **31**: 241–250.

Zander, U., Faust, A., Klink, B.U., de Sanctis, D., Panjikar, S., Quentmeier, A., *et al*. (2011) Structural basis for the oxidation of protein-bound sulfur by the sulfur cycle molybdohemo-enzyme sulfane dehydrogenase SoxCD. *J Biol Chem* **286**: 8349–8360.

Supporting information

Additional Supporting Information may be found in the online version of this article at the publisher's web-site:

Fig. S1. Genome scaffold lengths labeled by node # referenced in the text. Locations of specific homologous genes are indicated by boxes in their order on the scaffold (cyt-c: cytochrome c; sqr: sulfide quinone reductase; sr: sulfite reductase; sd: sulfide dehydrogenase; rhd: rhodanese; tsd: thiosulfate dehydrogenase; SoxABCDLXY: enzymes involved in the Sox pathway). Genes indicated by parentheses are second copies of genes with weaker affinities.

Fig. S2. Sequence alignment of thiosulfate dehydrogenase (tsd) homologous proteins. Included is the *A. vinosum* and Tint_2892 genes of the alignment in Denkmann *et al*. (2012), the closest match with the *T. thermophila* gene annotated as a hypothetical protein in *T. arctica*, and the gene from *T. thermophila* from this study. The heme-binding motifs are highlighted in grey; distal ligands are in blue, and the catalytic cysteine in red.

Fig. S3. Phylogenetic tree of the Gammaproteobacteria created in ARB based on a 16S rRNA gene alignment from the SILVA "All-Species Living Tree" Project (Munoz *et al*., 2011; Yarza *et al*., 2008). Sequences from *Thiomicrospira thermophila* strain EPR85 and *Thiomicrospira crunogena* XCL-2 were inserted using the ARB parsimony algorithm.

Table S1. Stoichiometry of all growth experiments. Polythionates (S_3O_6 and S_4O_6) were determined using cyanolysis. *Indicates S_2O_3 concentrations determined with the cyanolysis method. All other S_2O_3 concentrations were determined by ion chromatography.

Table S2. Stoichiometry of all abiotic control experiments. Polythionates (S_4O_6) were determined using cyanolysis. *Indicates S_2O_3 concentrations determined by the cyanolysis method. All other S_2O_3 concentrations were determined by ion chromatography. All experiments were performed at 35°C unless otherwise noted. Measurements below detection are indicated as b.d. and as n.a. if not analyzed.